Nat. Hazards Earth Syst. Sci. Discuss., 2, 7487–7506, 2014
www.nat-hazards-earth-syst-sci-discuss.net/2/7487/2014/
doi:10.5194/nhessd-2-7487-2014

Natural Hazards and Earth System Sciences
Discussions
Open Access

Ground-penetrating radar observations for estimating the vertical displacement of rotational landslides

C. Lissak[1,2], O. Maquaire[2], J.-P. Malet[3], F. Lavigne[4], C. Virmoux[4], C. Gomez[5], and R. Davidson[2]

[1]PRODIG, CNRS – UMR8586, Université Paris Diderot, Sorbonne-Paris-Cité Paris, Paris, France
[2]Laboratoire LETG-CAEN GEOPHEN, Géographie Physique et Environnement, CNRS – UMR6554, Université de Caen-Basse-Normandie, Esplanade de la Paix, 14032 Caen CEDEX, France
[3]Institut de Physique du Globe de Strasbourg, CNRS – UMR7516, Ecole et Observatoire des Sciences de la Terre, EOST/Université de Strasbourg, 5 rue Descartes, 67084 Strasbourg, France
[4]Laboratoire de Géographie Physique, CNRS – UMR8591, Meudon, France
[5]University of Canterbury, Natural Hazards Research Centre, Waterways: Centre for Freshwater Management, College of Sciences, Department of Geography, Private Bag 4800, 8140 Christchurch, New Zealand

Received: 13 November 2014 – Accepted: 19 November 2014 – Published: 12 December 2014

Correspondence to: C. Lissak (candide.lissak@univ-paris-diderot.fr)

Published by Copernicus Publications on behalf of the European Geosciences Union.

NHESSD

2, 7487–7506, 2014

Abstract

The objective of this paper is to demonstrate the applicability of Ground Penetrating Radar (GPR) for monitoring the displacement of slow-moving landslides. GPR data is used to estimate the vertical movement of rotational slides in combination with other surveying techniques. The experimental site is located along the Normandy coast (North East France) here several rotational landslides are continuously affected by a seasonal kinematic pattern (low displacement rates of 0.01 to 0.10 m yr^{-1}) and periodically by major acceleration events (high displacement of 1.0 to 7.0 m per event).

1 Introduction

Slow-moving landslides can present highly variable displacement fields. Typically, rotational landslides are confined by a circular basal slip surface and are affected by vertical movement upslope and horizontal movement downslope (Fig. 1). The direction and magnitude of the displacement components vary in space and time according to the bedrock geometry and the slope topography. In order to estimate the displacement rates at high accuracy (e.g. infra-centimetric), several geodetical ground-based techniques can be considered (Fig. 1) including GNSS, high-precision topographic levelling (Coltorti et al., 1985) and total station surveys (Tsai et al., 2012). These techniques, however, provide variable precisions (Travelletti et al., 2012). Topographic levelling is the most accurate technique for measuring the displacement in the vertical component with precision of the order of 1 mm; differential GNSS is the most precise technique for measuring the horizontal displacement (E–W and N–S components; Malet et al., 2002). However, in some landslide case studies, these classical investigation tools are not suitable or insufficiently precise because of difficult environmental conditions (dense vegetation, buildings), complex accessibility (private properties) or too small displacement rates. To overcome some of these difficulties, Ground Penetrating Radar (GPR) is used to provide precise information on the vertical motion of ground structures

NHESSD
2, 7487–7506, 2014

over a period of several years. GPR observations allow mapping horizontal and vertical discontinuities and fractures at the sub-surface (Deparis et al., 2007). The tracking of these discontinuities in time provides an indirect measurement of the subsidence of the buried ground structures. Over the last decade, GPR observations were frequently used in landslide research for identifying the geometry of the bedrock (Grandjean et al., 2000; Bichler et al., 2004; Sass et al., 2008), characterizing the pattern of sub-surface fractures (Deparis et al., 2007), and estimating the layering of buried structures (Gutierrez et al., 2011; Carpentier et al., 2012). GPR observations are limited to the analysis of hard rocks and coarse or consolidated sediments because of the attenuation of the radar signal in clay-rich material and in soils with a high saline groundwater content (Annan, 2005; Jeannin et al., 2006).

In our experiment, GPR observations are used for monitoring the vertical displacement of the "Cirque des Graves" (Fig. 2b) and the "Chant des Oiseaux" (Fig. 2c) landslides for the period 1980–2010 (Ballais et al., 1984; Flageollet et al., 1987; Maquaire, 1990). Since January 1982, the movements induced many damages and repairs of the road crossing the landslides. The landslide motion is complex and associates a seasonal kinematic regime (subsidence of a few centimeters per year) and an event-type kinematic regime (with major acceleration events of several decimeters per event).

The multiple repairs of the road pavement has created a succession of road structures characterized by variation in soil density. The evolution in time of this layering, which can be detected by GPR observations, is used to infer the vertical displacement rates. The geotechnical structure of the road is adapted to a good GPR signal-to-noise ratio as it associates a foundation layer and a pavement layer with gravel and compacted sand.

In this paper, we illustrate how the GPR can be used as a complementary tool to traditional geodetic measurements for estimating vertical displacement rates along cross-sections. We first detail the proposed methodology for detecting and locating the different road layers. Second, we interpret the position of the buried structures and quantify their displacement in time (for a period of 30 years). Finally, we compare the

NHESSD
2, 7487–7506, 2014

GPR-derived displacements to the displacements monitored at the surface with other surveying techniques.

2 Study area

The study area is located at the western margin of the sedimentary Paris Basin (Northern France) in Normandy. On the edges of the Pays d'Auge plateau (Fig. 2a), in a coastal area below 140 m a.s.l., several active landslides have induced frequent damages to the roads and buildings for the last twenty years. The two main unstable slopes are the "Cirque des Graves" landslide (Villerville; Fig. 2a and b) which is the largest, (47 ha; ≈ 20 m depth in 2012), most active and most documented landslide of the region (Maquaire, 1990; Lissak, 2012) and the "Chant des Oiseaux" landslide (Trouville; Fig. 2a and c) which is smaller in size (20 ha, ≈ 20 m depth in 2012).

2.1 Geology and geomorphology

The "Cirque des Graves" and the "Chant des Oiseaux" landslides are located on low elevation convex-concave slopes. They present a complex morphology with a succession of multiple and embedded rotational slumps (Fig. 1). Typical morphological features testifying the presence of circular slip surfaces are observed, such as scarps of various sizes (Fig. 2b and c), open fissures, small grabens and counter-slopes. The two landslides are delineated upslope by a major scarp (5–10 m high) cut in the Cenomanian chalk formation (Lissak et al., 2014), and downslope by a rocky reef in the Oxfordian sandstone formation. From the bottom to the top, the lithostratigraphic profile consists in Jurassic sedimentary rocks with superimposed strata of almost 10 m thick Oxfordian sandstone (plunging gently to the South-East at 15 %), Kimmeridgian marls (25 m thick), a layer of Albian sands (2–5 m thick) and Cenomanian chalk which thickness can exceed 50 m on the plateau (Fig. 2a).

NHESSD
2, 7487–7506, 2014

2.2 History of development

The "Cirque des Graves" and the "Chant des Oiseaux" slopes are continuously active landslides with displacement rates in the range 1–10 cm yr^{-1} on average. As a consequence of this slow movement, a continuous subsidence of the upper part of the landslides is observed causing small deformation of the road pavements and yearly repairs (Fig. 3). The landslides is also episodically affected by large acceleration as it was observed at the "Cirque des Graves" landslide in January 1982, February 1988, March 1995 and March 2001. During these events, displacements of up to several decameters and major changes of the slope topography (retrogression of the main scarp, creation of new secondary scarps) were observed, and major changes (Fig. 3b). As a consequence of these failures several houses and road sections were damaged or destroyed.

3 Methods

3.1 Displacement monitoring network

After the large failure event of January 1982 at the "Cirque des Graves" landslide, the authorities in charge of the road traffic installed a monitoring network on both sides of the RD513. The monitoring network consisted of four fixed observation points (PT 1-1′ at both sides of the cross-section S1; PT 2-2′ at both sides of the cross-section S2; Fig. 2a). The position of the points was measured every 3–5 months using total stations with a sub-centimeter accuracy. In 2008 and 2009, a network of 24 benchmarks was installed at the "Cirque des Graves" landslides to cover a larger area. Two cemented benchmarks were installed at the landslide boundary of the landslide (no. 407, no. 408; Fig. 2a) close to the previous observation point PT 1-1′. The position was measured by dGPS campaigns (Trimble R5) four times per year. The protocol consisted in 15 min observation time at each benchmark using a real-time kinematic mode; the position

NHESSD
2, 7487–7506, 2014

accuracy is estimated at 3 ± 3.5 cm for the east component, 6 ± 6.5 cm for the north component, and 6 ± 6 cm for the up component.

3.2 GPR acquisition and processing

For a non-invasive analysis of the subsurface, GPR measurements were acquired with a RAMAC GPR system (Mala Geoscience; Fig. 3) along 3 cross-section (S1, S2, S3; Fig. 2a) of 50–90 m length and 6 m wide. To prospect the entire width of the cross-sections, 4 to 5 parallel profiles (P1 to P17) are acquired (Fig. 3a).

Considering the field configuration (trees, presence of clay-rich formation in depth, high soil water content), a shielded low frequency antenna (dipole 500 MHz in a mono-static arrangement) was used for an optimal image resolution. With this configuration, the penetration depth does not exceed 4 m (Fig. 4a). The GPR observations were recorded with an in-line sampling interval of 0.05 m and a total time window of 105 ns. The GPR data was processed with the Reflex® software (Sandmaier, 1997) with a time sampling of 9666 MHz and a sampling rate of 1024. The processing chain consists of six steps (Fig. 4b). The inversion consists in the "Dewow" processing (1); this step is usually realized to correct and remove the very low-frequency components. The next step of processing (2) is the Time Gain process, using an energy decay (factor 0.6). Then a correction of start time (3) (T_0 ($z = 0$)) is applied to differentiate the air waves (which travels directly from the transmitter to the receiver in the air) and the ground waves in the soil surface. The data are then processed using a band pass Butterworth filter to improve the signal-to-noise ratio (4). The frequency bands chosen for filtering were 80–550 MHz. The topography effects are then corrected (5) by integrating the topographic profiles acquired by dGPS at several points along the cross-sections. Finally, a time-depth conversion is applied (Fig. 5).

NHESSD
2, 7487–7506, 2014

4 Results

The surface displacements are analyzed by combining GPR observations (Fig. 6) and surface geodetic measurements (levelling of the former topographic network, dGPS acquisition on the actual benchmark network; Fig. 7). The combination of these data provides a quantification of the total subsidence of the road RD513 crossed by the landslides between 1982 and 2010. The analysis provides also information on the major slope failure of January 1982 for which no direct measurements were available.

4.1 Interpretation of the Ground Penetrating Radar cross-sections

The GPR observations allow detecting different soil structures at the subsurface with successive high amplitude horizontal reflectors till depth of 6 m (Fig. 6). The horizontal reflectors can be interpreted as a significant contrast between two pavement layers with a different material composition or water content. The precision on the location in depth of the reflector is estimated at 15 cm.

In cross-section S1 (Fig. 6), the horizontal structure is disturbed at the distances 10 and 37 m by a reflector dipping steeply. It corresponds to the landslides boundaries. In this part of the cross-section, the number of detected layers increases with a thickening of the road structure. We can distinguish 2 units at the sub-surface: the "collapsed road" (1 m thick) and the "uncollapsed road" (maximum 3 m thick) which is affected by a continuous subsidence. Assuming a road structure with a thickness of 1 m according to the engineering plans, we can differentiate the road pavement of 1982, 1988, 1995 and 2001 (corresponding to the actual road level). The top of the 1982 road is observed between 1.80 and 2.30 m depth depending on the initial topography. The top of the 1988 road is located between 1.40 and 2.0 m in depth; the top of the 1995 road is located between 1.0 and 1.40 m depth.

A similar structure is observed along cross-section S2 (Fig. 6) located a few meters away. For this cross-section, the horizontal structure is disturbed at 22 and 70 m distance. The thickness of the collapsed road is asymmetric with a thickness of 4 m in

NHESSD
2, 7487–7506, 2014

the eastern part that progressively decreases westward. The top of the 1982 road is located at 3 m depth. The top of the 1988 road is at a maximum depth of 2.40 m and the top of the 1995 road is at a maximum depth of 1.40 m.

For the cross-section S3, located at the "Chant des Oiseaux" landslide (Fig. 6), this structure is also visible with a clear distinction between the "uncollapsed road" and the "collapsed road". Between 22 and 47 m distance, the thickness of the road exceeds 3 m. Only a few information on the landslide kinematic pattern was available for this landslide, as no major slope failure was precisely dated. Consequently we cannot define the year of the pavement. However, the determined depths are quite similar to the depths identified at the "Cirque des Graves".

4.2 Kinematics of the landslides over the period 1982–2010

The depths of the different layers identified on the GPR cross-sections are compared to the levelling data available for the period November 1982–April 1995. Figure 7 indicates a motion characterized by a constant displacement rate during 14 years and two major slope failures (February 1988, March 1995) with higher displacement rates. In between the two slope failures of May 1988 and April 1994, a subsidence of 0.25 m is measured at point PT 2-2′, corresponding to a subsidence rate of 2–3 cm yr^{-1}. At the contrary, during the slope failures, 30–40 cm of collapse are reported (Lissak et al., 2013).

Between 2008 and 2012, during a period of low landslide activity, the subsidence of the road was monitored by dGPS campaigns with a network of 24 benchmarks. The results of measurement (2009–2012) of only two of them are presented in this paper (Fig. 7). The up component (vertical) of the landslide movement is usually the most difficult to measure by dGPS because of the geometry of the satellite constellation (Malet et al., 2002). Consequently, the precision of the dGPS measurements is not sufficient to quantify accurately the displacement for 15 min short period acquisitions. Nevertheless, the recent activity of the landslides is clearly identifiable and can be measured through the monitoring of several fissures along the road. A subsidence rate of 1–2 cm yr^{-1} is defined for the period 2008–2012.

NHESSD
2, 7487–7506, 2014

The combination of geophysical and geodetic surveying techniques provides an estimation of the total subsidence of the slopes since 1982. The results include the first reactivation of the "Cirque des Graves" landslide for which no data was available before the GPR surveys. In this way, since January 1982, we can estimate a total collapse of the road comprised between 1.80 and 2.20 m at point PT 1-1′, and between 2.40 and 2.60 m for point PT 2-2′. These values integrate the seasonal activity of the landslide between 2 and 4 cm yr^{-1} and the 4 major slope failure with a major acceleration in January 1982 with 30–40 cm of collapse.

5 Conclusions

The use of the Ground-Penetrating Radar observations for assessing slope dynamics is not very frequent. This technique is usually used to gain knowledge on the internal structures of the slope or to obtain some petrophysical properties of the discontinuities.

Indeed, in our application, the GPR observations were used to detect the total subsidence of a road crossing two slow-moving landslides located along the Normandy coast. The observations also provided also valuable information on the dynamics of the landslide for the last 30 years. The geophysical data are completed by surface displacement measurements. At the "Cirque des Graves" landslide, geodetic measurements were performed between 1982 and 1995 and between 2009 and 2012 to estimate the vertical component of the movement. The results indicate a total collapse comprised between 1.8 and 4.0 m since 1982 for the two landslides. These results consider the seasonal pattern of the vertical movement associating a continuous displacement rate of 2–4 cm yr^{-1} and 4 major slope failures with displacement up to several decimeters per event.

GPR acquisition and data processing is potentially easy for sub-surface analysis; however this kind of investigation is highly constrained by the overhead wave reflections in complex geological structures, clay-rich material, and woody soils. Consequently, not so many slopes were investigated with this technique. This is the reason why our anal-

NHESSD
2, 7487–7506, 2014

ysis was focused in the upslope part of the landslides, along the road where the a good signal-to-noise was available because of the road pavement structure. The results of our study show that this field configuration was adequate for using radar pulses to image the subsurface and that GPR observations can be used as complementary tool for analysing landslide dynamics.

Acknowledgements. This research was funded by the ANR RiskNat project "SISCA: Système intégré de Surveillance de Crises de glissements de terrain argileux" (2009–2013) of the Agence Nationale de la Recherche (ANR-08-RISK-0009) and the Project "CPER GR2TC: Gestion des Ressources, Risques et Technologie du domaine Côtier" (2007–2013). The permanent GNSS system and the automated processing of the observations were setup by the OMIV-EOST Unit at University of Strasbourg as part of the French Observatory on Landslide. We also thank the LETG-Caen Geophen laboratory team for installing the device in the field.

References

Annan, A. P.: GPR methods for hydrogeological studies, in: Hydrogeophysics, edited by: Rubin, Y. and Hubbard, S. S., Water and Science Technology Library, Springer, the Netherlands, 185–213, 2005.

Ballais, J.-L., Maquaire, O., and Ballais, H.: Esquisse d'une histoire des mouvements de terrain dans le Calvados depuis 2 siècles, in: Actes du Colloque "Mouvements de Terrain", edited by: Documents du BRGM, 83, BRGM, Orléans, 476–483, 1984.

Bichler, A., Bobrowsky, P., Best, M., Douma, M., Hunter, J., Calvert, T., and Burns, R.: Three-dimensional mapping of a landslide using a multi-geophysical approach: the Quesnel Forks landslide, Landslide, 1, 29–40, 2004.

Carpentier, S., Konz, M., Fischer, R., Anagnostopoulos, G., Meusburger, K., and Schoeck, K.: Geophysical imaging of shallow subsurface topography and its implication for shallow landslide susceptibility in the Urseren Valley, Switzerland, J. Appl. Geophys., 83, 46–56, 2012.

Coltorti, M., Dramis, F., Gentili, B., Pambianchi, G., Crescenti, U., and Sorriso-Valvo, M.: The December 1982 Ancona landslide: a case of deep-seated gravitational slope deformation evolving at unsteady rate, Z. Geomorphol., 29, 335–345, 1985.

NHESSD

2, 7487–7506, 2014

Deparis, J., Garambois, S., and Hantz, D.: On the potential of ground penetrating radar to help rock fall hazard assessment: a case study of a limestone slab, Gorges de la Bourne (French Alps), Eng. Geol., 94, 89–102, 2007.

Flageollet, J.-C., Gigot, P., Helluin, E., and Maquaire, O.: Studies on landslides in Normandy (France) in view of their occurrence probability, in: Proceedings of the 5th International Conference and Field Workshop on Landslides, ANZSLIDE 87, Australia & New Zealand, Christchurch, New Zealand, 225–233, 1987.

Grandjean, G., Gourry, J.-C., and Bitri, A.: Evaluation of GPR techniques for civil-engineering applications study on a test site, J. Appl. Geophys., 45, 141–156, 2000.

Gutierrez, F., Galve, J. P., Lucha, P., Castañeda, C., Bonachea, J., and Guerrero, J.: Integrating geomorphological mapping trenching InSAR and GPR for the identification and characterization of sinkholes. A review and application in the mantled evaporite karst of the Ebro Valley (NE Spain), Geomorphology, 104, 144–156, 2011.

Jeannin, M., Garambois, S., Jongmans, D., and Grégoire, C.: Multi-configuration GPR measurements for geometric fracture characterization in limestone cliffs (Alps), Geophysics, 71, B85–B92, 2006.

Lissak, C.: Coastal Landslides of the Pays d'Auge (Calvados): Morphology, Functioning and Risk Management, PhD thesis, University of Caen, Caen, France, 312 pp., 2012.

Lissak, C., Puissant, A., Maquaire, O., and Malet, J.-P.: Analyse spatio-temporelle de glissements de terrain littoraux par l'exploitation de données géospatiales multi-sources, Revue Internationale de Géomatique, 23, 199–225, 2013.

Lissak, C., Maquaire, O., Malet, J.-P., Bitri, A., Samyn, K., Grandjean, G., Bourdeau, C., Reiffsteck, P., and Davidson, R.: Airborne and ground-based data sources for characterizing the morpho-structure of a coastal landslide, Geomorphology, 217, 140–151, 2014.

Malet, J.-P., Maquaire, O., and Calais, E.: The use of Global Positioning System techniques for the continuous monitoring of landslides: application to the Super-Sauze earthflow (Alpes-de-Haute-Provence, France), Geomorphology, 43, 33–54, 2002.

Maquaire, O.: Les mouvements de terrain de la côte du Calvados: recherches et prévention, Documents du BRGM, 197, BRGM, Orléans, France, 1990.

Sandmeier, R.: Reflexw Help Notes, Sandmeier Software, available at: http://www.sandmeier-geo.de (last access: December 2014), 1997.

NHESSD

2, 7487–7506, 2014

Sass, O., Bell, R., and Glade, T.: Comparison of GPR, 2-D-resistivity and traditional techniques for the subsurface exploration of the Oschingen landslide, Swabian Alb Germany, Geomorphology, 93, 89–103, 2008.

Tsai, Z.-X., You, G. J.-Y., Lee, H.-Y., and Chiu, Y.-J.: Use of a total station to monitor post-failure sediment yields in landslide sites of the Shihmen reservoir watershed, Taiwan, Geomorphology, 139–140, 438–451, 2012.

Travelletti, J., Delacourt, C., Allemand, P., Malet, J.-P., Schmittbuhl, J., Toussaint, R., and Bastard, M.: Correlation of multi-temporal ground-based optical images for landslide monitoring: Application, potential and limitations, ISPRS J. Photogramm., 70, 39–55, 2012.

NHESSD

2, 7487–7506, 2014

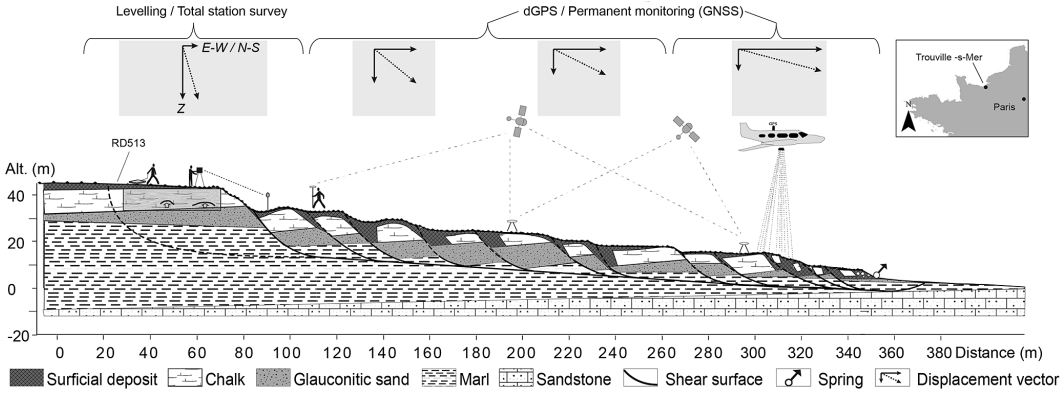

Figure 1. Typical cross-section of a complex rotationnal landslide (example of the “Cirque des Graves” landslide) with indication on the distribution of displacement per units from upslope to downslope and on the appropriate displacement monitoring techniques.

NHESSD
2, 7487–7506, 2014

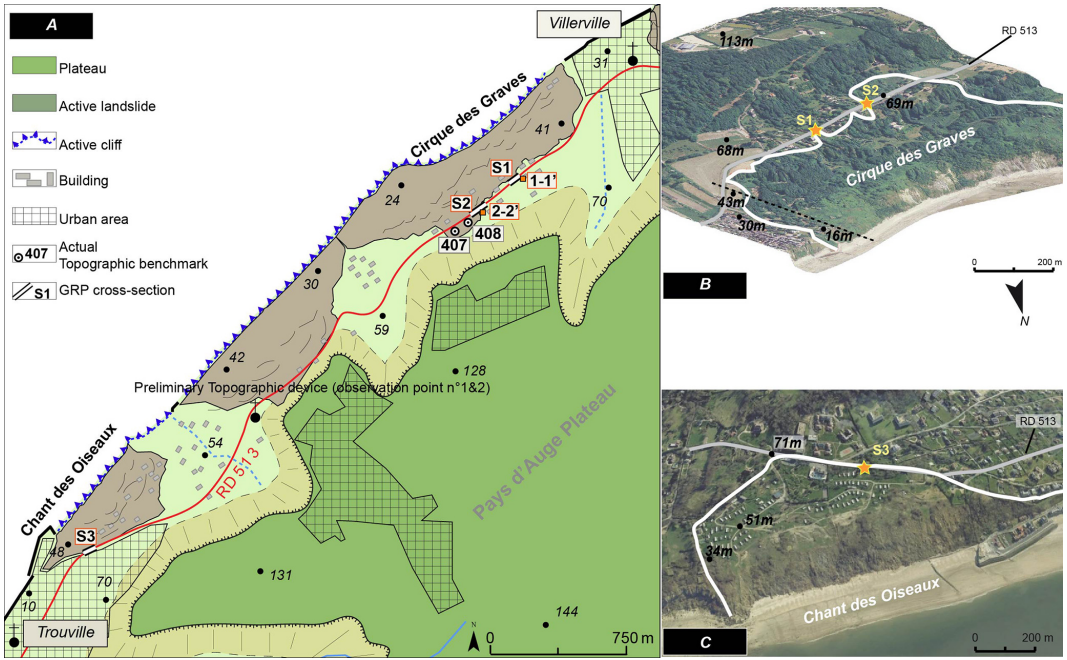

Figure 2. Morphology of the studied landslides. **(a)** Active landslides along the coast between Trouville and Villerville and location of the field investigations. **(b)** Aerial images 2006 of the "Cirque des Graves" landslide at Villerville. **(c)** Satellite view (Image 2014© Google Earth) of the "Chant des Oiseaux" landslide at Trouville.

NHESSD
2, 7487–7506, 2014

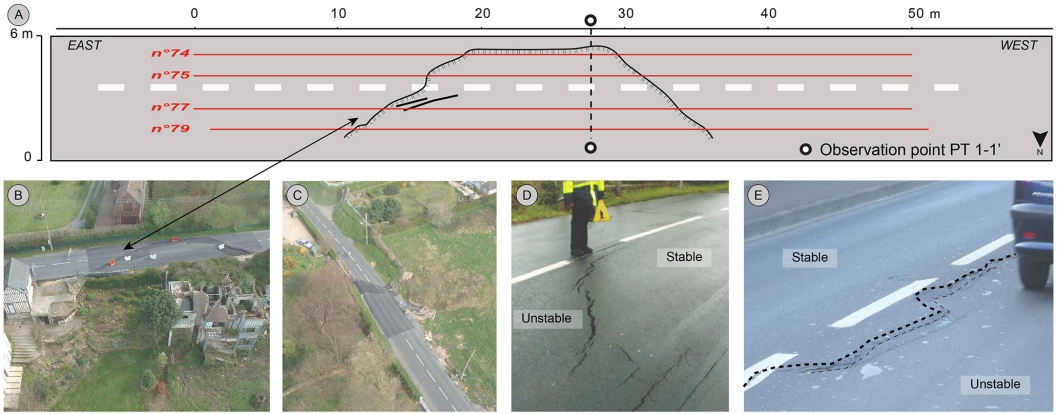

Figure 3. Damages observed along the RD513 road and strategy of GPR data acquisition. **(a)** Example of a GPR cross-section (cross-section S1) along the deformed road (multiple parallel profiles are acquired). **(b)** Oblique picture of the road collapse at the observation point S1 after the March 2001 failure. **(c)** Oblique picture of the road collapse at the observation point S2 after the March 2001 failure. **(d)** Fissures observed along the road at point S2 in 2012. **(e)** Fissures along the road at the point S3 in 2009.

NHESSD
2, 7487–7506, 2014

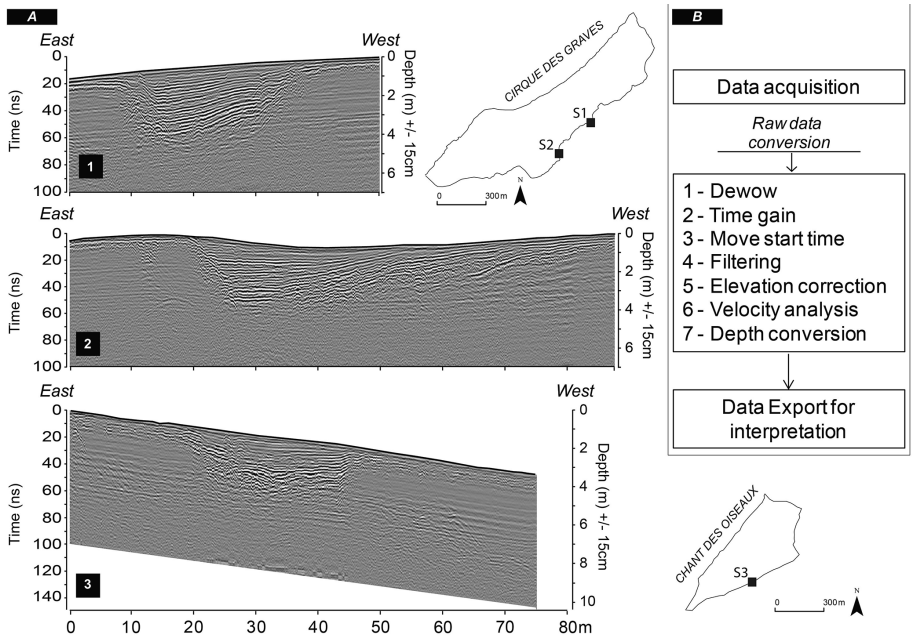

Figure 4. Example of raw GPR observations. **(a)** Cross-sections S1 and S2 at the "Cirque des Graves" landslide and cross-section S3 at the "Chant des Oiseaux" landslide, **(b)** GPR observations processing chain.

NHESSD
2, 7487–7506, 2014

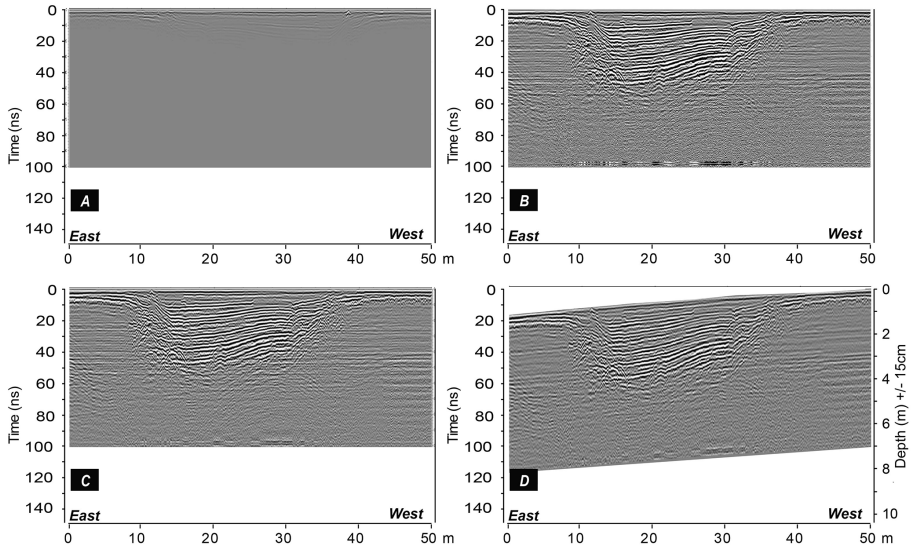

Figure 5. Illustration of the processing chain applied to the GPR observations data acquired with a 500 MHz dipole shielded antenna at profile S1. **(a)** Raw data, **(b)** processed data using gain, **(c)** processed data after band pass filtering, **(d)** conversion time-depth.

NHESSD
2, 7487–7506, 2014

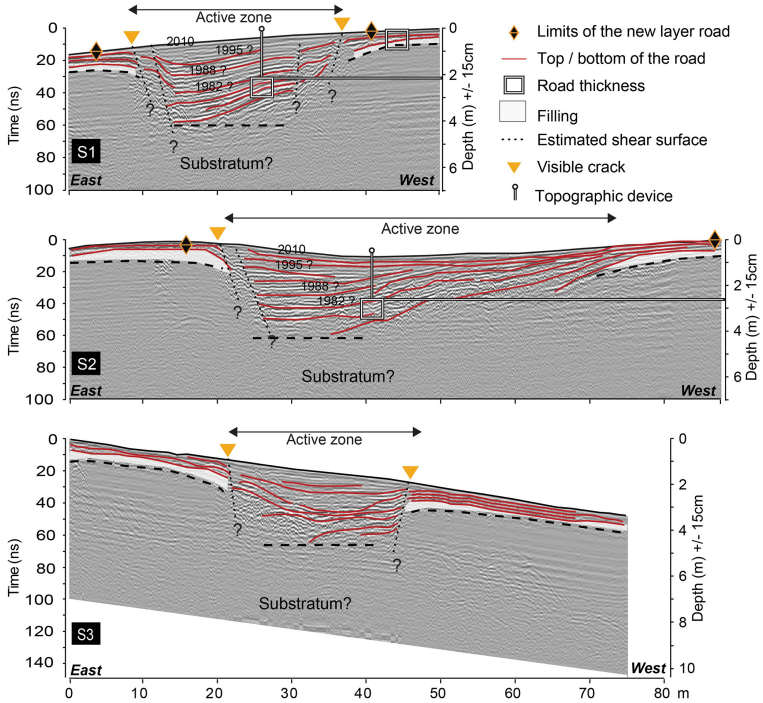

Figure 6. Interpretation of the Ground-Penetrating Radar observations for cross-sections S1, S2 and S3.

NHESSD
2, 7487–7506, 2014

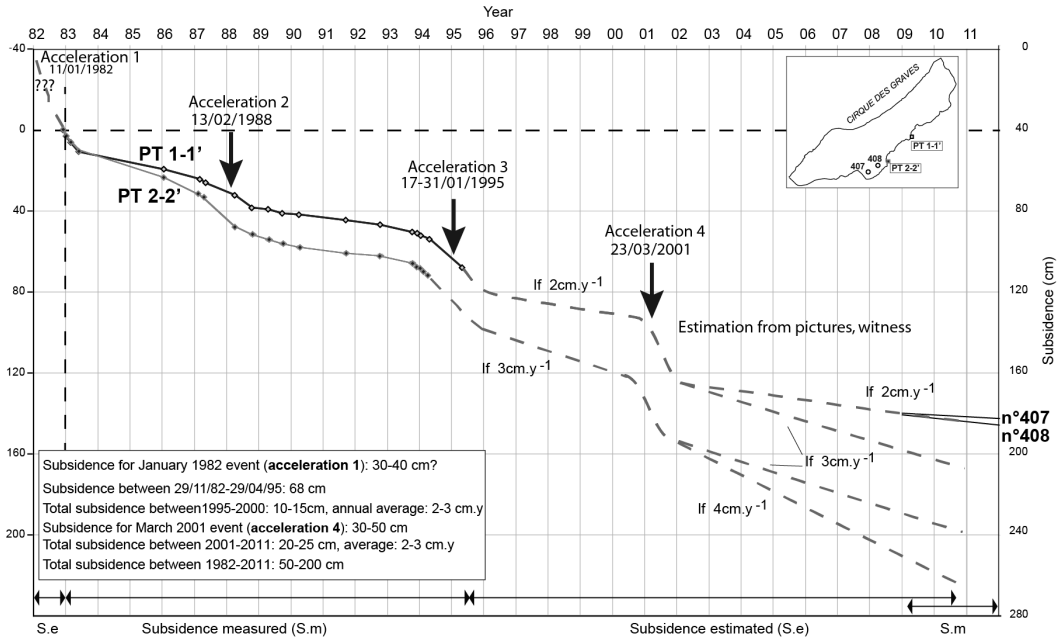

Figure 7. Subsidence of the road measured and estimated between 1982 and 2011.

NHESSD
2, 7487–7506, 2014